International Research Journal of Geology and Mining (IRJGM) (2276-6618) Vol. 4(3) pp. 84-100, April, 2014
DOI: http:/dx.doi.org/10.14303/irjgm.2013.028
Available online http://www.interesjournals.org/IRJGM


*Review*

# Deformation history of Nugrus- Sikiat Belt, South Eastern Desert, Egypt; implication for Tectonic Environment

**[*1, 2]Ibrahim WS, [2]Mostafa MS, [2]Ibrahim ME, [1]Watanabe K and [3]Soliman FA**

[1]Department of Earth Resources Engineering, Faculty of Engineering, Kyushu University, Fukuoka 819-0395, Japan
[2]Nuclear Materials Authority, Cairo, Egypt
[3]Suez of Canal University, Ismailia, Egypt
*Corresponding Author Email: W-Ibrahim@mine.kyushu-u.ac.jp

**Abstract**

**The Nugrus –Sikait belt comprises metamorphic exposures which are mainly represented by two nappes; upper nappe (dismembered ophiolitic rocks) and lower nappe (pelitic, para-amphibolite and cataclastics assemblages) separated by ophiolitic mélange. Intra-cratonic association (granitic and gabbroic rocks) intrudes these rock associations. Styles, overprinting relationships between the different structural fabrics, where each rock assemblages show its own tectonic print revealed that Nugrus-Sikait belt underwent five distinct episodes of deformation (from D1to D5). Compression event (D1) with NW-SE to NNW-SSE $\sigma 1$ trend. E-W thrust faulting and forming E-W isoclinal folds (Df1). Compression event (D2) with NE-SW to ENE-WSW $\sigma 1$ trend. NW-SE thrust faulting and forming NW-SE folding (Df2). Transpressonal sinistral shearing (D3) with NW-SE to NNW-SSE$\sigma 1$ trend including top-to-NW oblique-slip shearing and NNE-SSW dextral strike-slip shearing led to development of the Nugrus-Sikait ductile shear zone and formed NNW-SSE folding (Df3). This event associated with emplacement of granitic intrusions, which cause folding around horizontal N-S direction (Df4). Extensional event (D4) with NE-SW to ENE-WSW $\sigma 3$ trend deformation probably related to exhumation of the complex with NNW-SSE normal and strike-slip faulting. Extensional event (D5) with NNW-SSE to N-S $\sigma 3$ trend restricted to the alkali feldspar granite. ENE-WSW to E-W normal faulting, this event associated with emplacement of post granitic dikes and veins. The tectonic evolution of the NSB can place important insights into a proposed tectonic model suggesting a back-arc basin tectonic environment. The basin was formed as faulted bounded basin controlled mainly by E-W and N-S trending.**

**Keywords:** Tectonics, Structures, Paleostress field, Folding, Nugrus-Sikait.

## INTRODUCTION

The Nugrus –Sikait belt (NSB), located within W. El Gemal environs, and represents the southeastern continuation of Wadi Hafafit Culmination (WHC). The WHC as well as NSB attracted the attention of many authors among themHashad and Hassan (1959),Basta and Zaki (1961),Hassan (1964 and 1973), Hashad et al. (1972), El Shazly and Hassan (1972), Bugrov et al. (1973), Sabet et al. (1976), Stern (1981), El Gaby (1983), El Bayoumi (1984), El Gaby et al.(1984), Hegazy (1984), Stern and Hedge, (1985), El-Gaby et al.(1988), Hilmy et al.(1990), Takla et al. (1992), Al Filali et al. (1993), El Ramly et al. (1993), Saleh (1998), Assaf et al. (2000), Ibrahim et al. (2000), Fowler and El Kalioubi (2002), Ibrahim et al. (2004), Rashed (2006) and Ibrahim et al. (2007a, bandc). The NSB is structurally located between the southern and central Eastern Desert domains (Figure 1), where the low-angle thrust zone, Nugrus Thrust, represent a zone of discontinuity between the two domains of the Eastern Desert (Stern and Hedge, 1985). This thrust fault localizes the limit between the medium metamorphic grade associations and the low metamorphic grade ophiolitic melange assemblage at the study area.

The studied area is a Precambrian basement terrain constituted of different lithological assemblage of igneous and metamorphic rocks. Most of these rocks are highly deformed which is featured by the frequent presence of

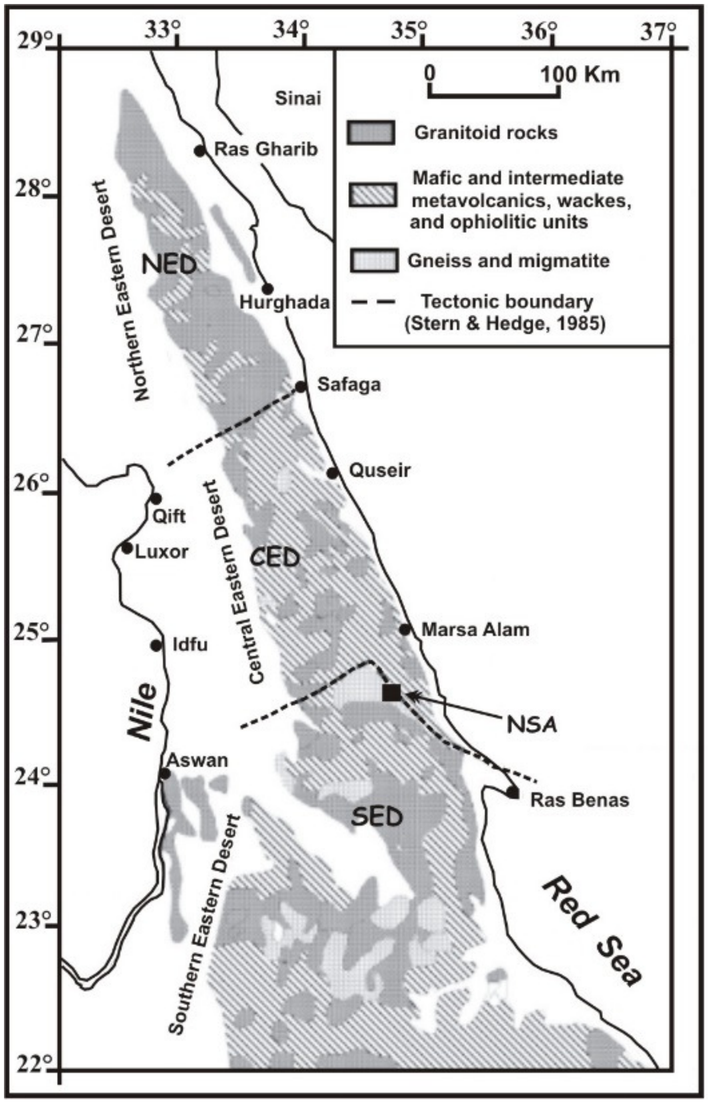


**Figure 1.**Generalized geological map of the Eastern Desert of Egypt showing the distribution of the basement rocks and the location of NSA with respect to the limits between the basement subdivisions, Southern Eastern Desert (SED), Central Eastern Desert (CED) and Northern Eastern Desert (NED) (from Stern and Hedge, 1985)

multiple mesoscopic structures.

On the other hand, Nugrus-Sikaitbelt is very rich in various economic mineralization (U, Th, Nb, Ta, Zn, Be, Sn, Cu, Ga and REEs). That makes this area as one of the most important and promising mineral resources areas in the Eastern Desert of Egypt.

The relation between igneous, metamorphic rocks as well as shear zones is important as a mean of determining the history of the deformational events of the study area that make up an orogenic system and configure its structural pattern. In particular, measuring the structural fabric pattern of geologic bodies in the field studies can help to establish the link between magma emplacement and tectonics.

This paper attempts to characterize, deduce, analyze and reconstruct the tectonic setting that controlling the structure pattern of the Precambrian crystalline rocks throughout NSB using the ductile and brittle deformation analysis techniques.

## Geological Setting

Based on the detailed field studies, the lithological associations found in NSB comprise two nappes; upper nappe (ophiolitic rocks) and lower nappe (pelitic, para-amphibolite and cataclastics assemblages) separated by ophiolitic mélange. These rock associations are latterly

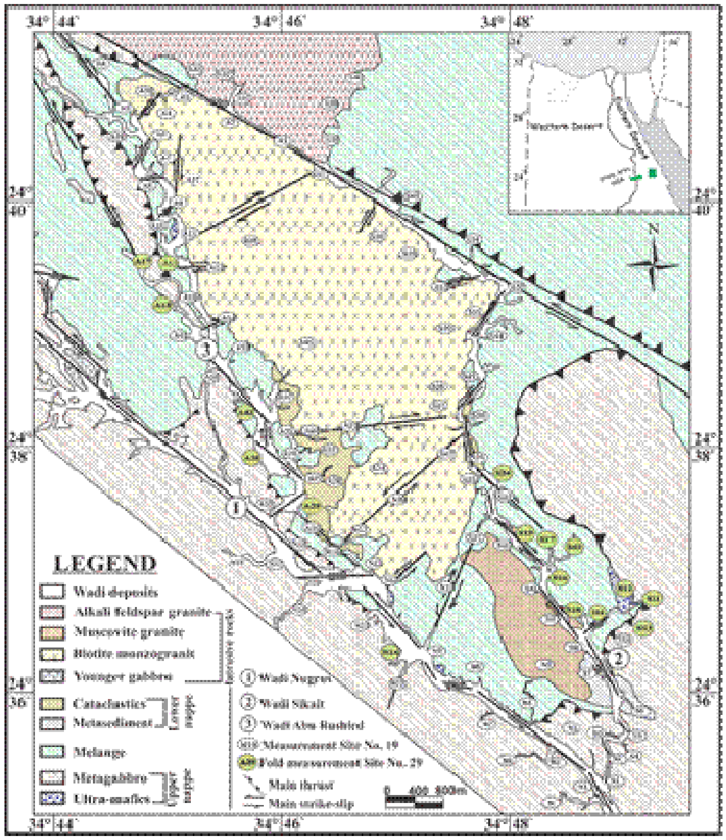


**Figure 2.**Detailed geologic map of Nugrus-Sikait Belt (NSB), showing the regional structural lines, the main wadis as well as the investigated sites distribution among the different rock types

intruded by granitic and gabbroic rocks (Figure 2).These rocks show gradual variation from low grade schist facies at the upstream of W. Nugrus (epidote and chlorite facies), thorough the medium grade amphibolite facies (W. Abu Rusheid and downstream of W. Nugrus) to high grade amphibolite facies in tectonic mélange along W. Sikait (staurolite– kyanite–sillimanite facies).

The NS Brock associations are cut by various dykes and veins that comprise various lamprophyre dykes except the last two phases of granites (muscovite and alkali feldspar granites) which are mostly cut by various quartz and pegmatitic veins. The litho-stratigraphic rock types are summarized on Table (1).

The contact between the first two rock assemblages is a structural contact represented by a regional NW-SE trending thrust belt dipping due NE direction whereas the intrusion of the granitoid pulses are controlled mainly by the NW-SE, NE-SW and N-S to NNW-SSE structural trends. In addition to that, some of these structural trends were associated with or responsible for the encountered folding in NSB that exhibits asymmetric varied geometries and axial plane orientations including buckle, chevron, sheath and kinking folds. In terms of interlimb angle they range between open to isoclines, and in terms of axial plane orientation they include gently inclined to almost recumbent folds whereas the interference patterns were recorded in some exposures.

## Deformation Analyses

NSBwas the object of intensive detailed systematic analyses of the structural fabrics e.g. foliation, lineation, folds, fault populations, joints, sense of movement and shear criteria, etc. The field measurements (more than 14,000 measurements) were collected throughout 109sites distributed in almost all the outcropping rock types in NSB (Figure 2).For each site, attention was paid to chronological criteria, overprinting relations, cross-cut relationships between fault and fracture systems.

The superposition of different movement marks slickenside lineation on a single fault plane, the reactivation of the pre-existing fault planes due to later on stress fields as well as fault geometry with respect to foliation planes and folding (fault-fold relationships) in order to differentiate and then categorize the succession

**Table 1.**Compiled litho-stratigraphic rock types of NSB

| | Rock types | Composition and Description | Geologic Setting | Occurrences |
|---|---|---|---|---|
| | Post granitic dikes and veins | Various types of dykes(lamprophyre and hornblendite) and veins (pegmatite andquartz)cut through the study area | Lamprophyre dikes cut all the rock units at NSB except the muscovite and alkali feldspar granites which are mostly cut by quartz and pegmatite veins. | Dikes and veins are distributed among all the rock units at NSB |
| Intrusive rocks | Alkali feldspar granites | Highly weathered granites composed of quartz, K-feldspar, plagioclase andcuts through the muscovite granite | | The right upstream side of both W. Sikait and W. Abu Rusheid intruding along the contact between the ophiolitic mélange and the biotite monzogranites and as offshoots along W.Nugrus |
| | Muscovite monzo granites | Composed of quartz, K-feldspar, plagioclase and muscovite, commonly contain xenoliths of mafic rocks and abundant garnet crystals | The emplacement of granitic plutons in the study area is controlled by two basic structural trends (NW-SE and E-W). To the south the pluton is surrounded by layered meta gabbros thrusted over ophiolitic mélange. | Occurs as white small masses along W. Sikeit, W. Nugrus and north of W. Abu Rusheid and as emplacing dike-like bodies injected into the biotite monzo granites |
| | biotite monzogranites | Composed mainly of quartz, plagioclase, feldspars, and biotite. | | Represent 70% of granitic rocks in the study area. Exposed to the north east of W. Abu Rusheid and upstream of W. Sikait |
| | Younger Gabbros | Coarse-grained gabbroid rocks comprise olivine gabbro and hornblende gabbro with gradational contacts | The emplacement of gabbroid rocks elongate through the same NW-SE structural trend | Cover a total area about 4 $km^2$, to the NW of NSB |
| | Cataclastics | Include protomylonites, mylonites, ultra mylonites and silicified ultra mylonites (quartzite) with gradational contacts. | Highly foliated, the intercalations between the proto mylonite and mylonite rocks are common manifesting the sedimentary origin.The ophiolitic mélange are thrusted over the cataclastic rocks. | Exposed at eastern side of W. Abu Rusheid covering about 3$km^2$and at eastern side of W. Sikait as small area (0.5$km^2$) forming low land terrain. |
| Lower nappe | para-amphibolites | These rocks are fine- to medium-grained and shows greenish grey to deep green color and composed mainly of hornblende, plagioclase and biotite | Display well defined foliation with relics of primary bedding. | Exposed only at the eastern side of W. Abu Rusheid covering a small area. |
| | metapelites | Composed mainly of Biotite schist and hornblende schist. | Display relics of primary bedding, foliations, and laminations, minor and macro-folding and are intruded by biotite granite and muscovite granites. | Cover the downstream of W. Sikait on the two sides. |
| | | ▼ ▼ ▼ ▼ ▼ ▼ ▼ | NW-SE Thrust contact | ▼ ▼ ▼ ▼ ▼ ▼ ▼ ▼ |
| | Ophiolitic mélange. | Composed mainly of Mélange matrix (mainly schists) that encloses abundant fragments of meta-periodotite, meta-pyroxenite and ortho-amphibolites of variable sizes and dimensions. The matrixesare represented by wide varieties (talc schist, quartzo-feldspathic schist, garnet-mica schist, tourmaline-garnetiferous-biotite schist, graphite schist and sillimanite schist). | The schists are the result of regional metamorphism of pelitic and psammo-pelitic sediments. These rocks are highly foliated and featured by the frequent presence of folds, boudinaged quartz and pegmatite lenses extending parallel to the foliation planes. E-Wand NW-SE Thrust contacts | Biotite schists are forming the greatest part of the schists in the study area and the main rock unit of Gabal Sikait, Talc schist is located to the east of W. Sikait, Tremolite-actinolite schists located near the contact with granitic rocks at W. Abu Rushied with related beryl occurrences, Garnetiferous hornblende-biotite schists on eastern side of W. Sikait and middle of W. Abu Rushied and Graphite schists as thin bands at middle and end of W. Sikait |

**Table 1.**Continuation

| | | | | |
|---|---|---|---|---|
| Upper nappe (dismember ophiolite) | Metagabbros | Exhibit a wide variation in colors, varying from dark grey to dark green in color. These rocks are characterizes by well-developed layering which reflect varying in composition in mafic and light minerals. The ophiolitic metagabbros are observes in sheeted mass overlying the ophiolitic mélange<br>▼ ▼ ▼ ▼ ▼ ▼ ▼ | The metagabbros are tholeiitic, high alumina, high–Ti ophiolite and equivalent to oceanic gabbros and back–arc basin<br>**E-W Thrust contact**<br>▼ ▼ ▼ ▼ | Represent the most predominant rock unites within the studied area where they are covering the eastern and southern parts of the study area.<br>▼ ▼ ▼ ▼ ▼ ▼ ▼ ▼ |
| | Meta-prediotites | Light brown color, soft, compact, soapy with the development of foliation in some places. Meta-peridotites are mostly highly serpentinized and in many places transformed into talc-carbonates, cream-color rocks. | Characterized by tholeiitic, high–Ti ophiolite, equivalent to metamorphic peridotites and ultramafic cumulate of low temperature Alpine type. | W.Nugrus, W.Sikait and W.Abu Rushied |

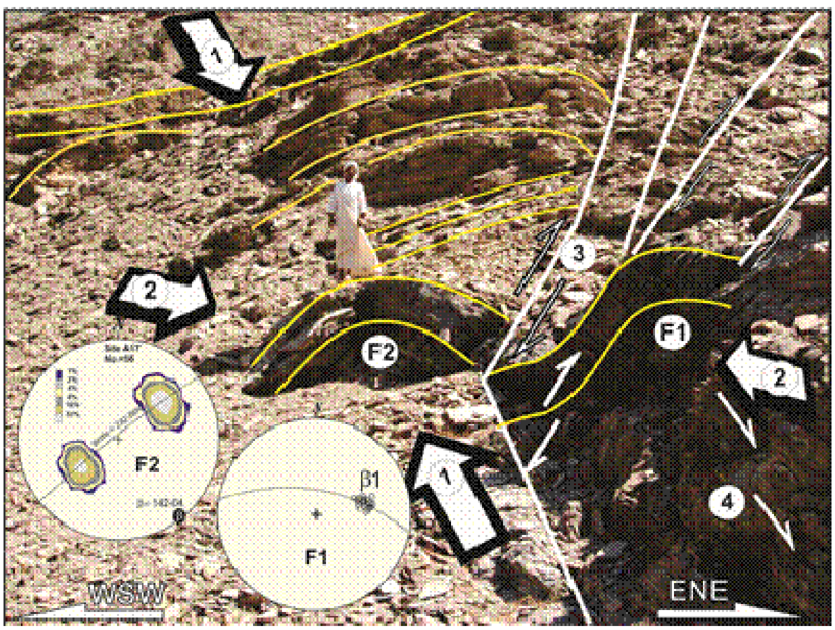


**Figure 3.**Chronological criteria; example of relative chronology used in dating the tectonic events in NSB.1st F1 fold system developed in metagabbroic bands with E-W trending fold axis, 2nd F2 isoclinals folds with NW-SE running fold axes, 3rd right lateral displacement along NNW-SSE strike-slip fault system and 4thENE-WSW dip-slip normal fault system

of the deformational events.

The analysis of these structural elements allowed the determination of both local and then regional orientations of the principal paleo-stress axes and establishing some relative chronologies (Figure 3). The results have been synthesized in order to reconstruct a schematic timing of the paleo-stress field evolutions that in turns allow defining the tectonic and geodynamic evolution.

## Ductile deformation analyses

The different rocks behave differently under stress; some rocks when subjected to the same stress will be fractured or faulted while others will be folded or recrystallized and foliated during deformation and/or dynamic metamorphism. The higher in temperature (i.e. the deeper within the crust), the more likely that ductile

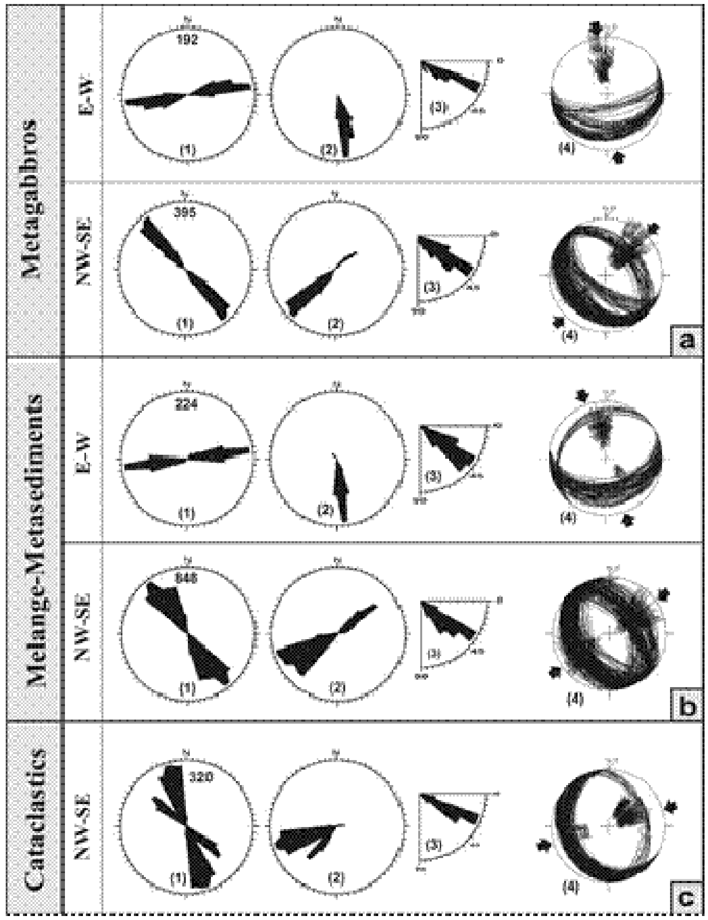


**Figure 4.**Foliation data representations as rose diagrams (1= strike, 2=dip direction, 3= dip angle and 4=lower hemisphere stereographic projection, NSB. (a. metagabbros, b. mélange - metasediments and c. cataclastics)

mechanism dominates over brittle mechanisms in controlling the style of deformation. Folding, mineral lineation and foliation in the metamorphic exposure rocks in Nugrus –Sikait belt are the most remarkable ductile deformational fabrics.

Detail studies of the ductile deformational fabrics was carried out among17 sites distributed along the metagabbros, mélange, metasediments and cataclasics exposures, where foliations, folding and refolding are well developed. More than 2,000measurements of foliation, lineaments and fold axes have been collected so that 587 measurements in metagabbros, 1,072 measurements in mélange and metasediments and 420 measurements in cataclastics. These measurements have been categorized and analyzed according to their trend distribution in each lithological type. Each system of foliation has been analyzed to deduce its principal compression direction with the help of the stereographic projection software packages GEOrient version 9.4 and Tector, Angelier (1989, 1990 and 1994).

**1) Foliations**

The metagabbro sets of foliations are arranged according to E-W and NW-SE main striking trends, suggesting N-S and NE-SW trending compression (Figure 4a).The mélange and metasediments sets of foliations are arranged due to ENE-WSW and NW-SE directions, reflecting NNW-SSE and NE-SW compressional trends (Figure 4b).The cataclastics set of foliations are oriented due to NW-SE to NNW-SSE general trend, revealing a compressional trend around the NE-SW direction (Figure 4c). Accordingly, it is believed that the NE-SW compression trend is post to and/or associated with cataclastics, whereas the N-S compression is the oldest one and restricted to metagabbros and or mélange.

**2) Folding**

At NSB, folding are restricted to the foliated layered

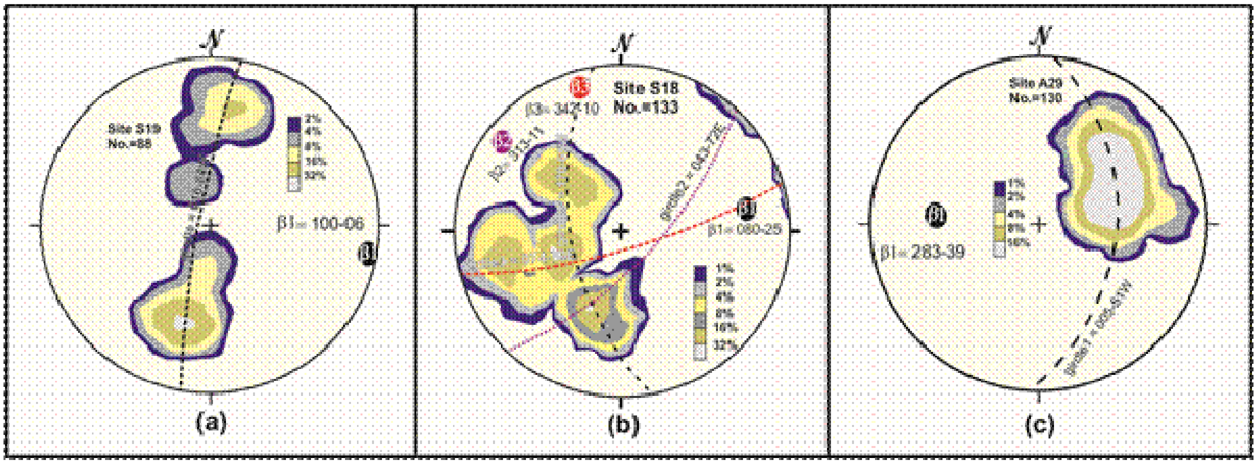


**Figure 5.**Density-contoured lower hemisphere Schmidt net stereograms of structural data, sites; S19, S18 and A29 Shading for all stereograms are from lowest to highest concentration representing poles to foliation measurements (a, b and c) for the E-W folding. Remark the impact of NW-SE folding then NNW-SSE folding (b)

metagabbros, mélange, metasediments and cataclastic rocks and are generally localized around and/or associated with the thrust belt sheet around W. Nugrus and W. Sikait, where the 17 sites of fold measurements are located (Figure 2).

These folds exhibit varied geometries including buckle, chevron, sheath and kinking folds with interlimb angle ranging from 30$^o$ to 120$^o$ reflecting open to tight fold types which are agreement with Marshak and Mitra (1988). In additional to that, the axial plane inclinations are found to be ranging widely from 0$^o$ to 90$^o$ at Nugrus – Sikait belt, where upright, overturned and recumbent folds were recorded. Generally, the folds as well as foliation measurement analyses categorized four sets of folding which fold axes trended E-W, NNW-SSE, NNE-SSW and NW-SE with minor N-S ones (Figures 5, 6 and 7). Later on, these fold sets have been dislocated by an intense strike slip deformational regime (Figure 3).

**a) E-W Folding**

The E-W set of folding is characterized by cylindrical geometry, where the fold axes are plunging gently in E and W and run in E-W direction (Figure 5). The impact of the later fold sets is shown in Figures 5 and 6, where the interference fold pattern has been clearly recorded (Figure 6). This set of folding reflects an axis of shorting oriented around the N-S direction. In many sites, as shown in Figure (6), the E-W fold set has been refolded either during the NW-SE phase of folding and/or the NNW-SSE one (Figure 5; b).

Accordingly, E-W set of folds was considered as the oldest phase of folding (Df1) in NSB and represent an initial phase of shortening with an axis oriented around the N-S direction.

**b) NW-SE Folding**

Folds of NW-SE oriented fold axes (Figure 7) are widely recorded in the study area. Generally, this set was developed as asymmetric folds ranging from normal upright to overturned with different styles and geometries (Figures 6 and 7).

The detailed field observations recorded the association between this set of folds and the NW-SE thrust fault system, i.e. it is related to the same event of deformation (Figure 8). The interpretations of the shape of the folded rock types and their internal structure as well as the relative field chronological data suggest a second phase of folding (Df2) defined by NW-SE oriented fold axes (Figure 6).

**c) NNW-SSE Folding**

Folds of NNW-SSE oriented fold axes (Figure 9) are widely recorded as intrafolial event developed due to either coaxial strain or shear folded line strain forming discrete as well as zonal crenulations and kinking. Generally, this set has asymmetric geometry as tight to isoclinal folds, with axial planes approximately parallel to the plane of the foliation, and hinges lying at a small angle to the local extension lineation. These folds are well developed, especially in the meta-gabbro and mélange.

The folds of this set have been regarded either around or associated with a right lateral oblique slip dislocation system of regional scale that parallel to and/or at small angle with the NW-SE running thrusts(Figure 10c). Moreover, the relative field chronological fold-fold relationship between the NNW-SSE set of folds and either the E-W or the NW-SE ones reveals that both E-W

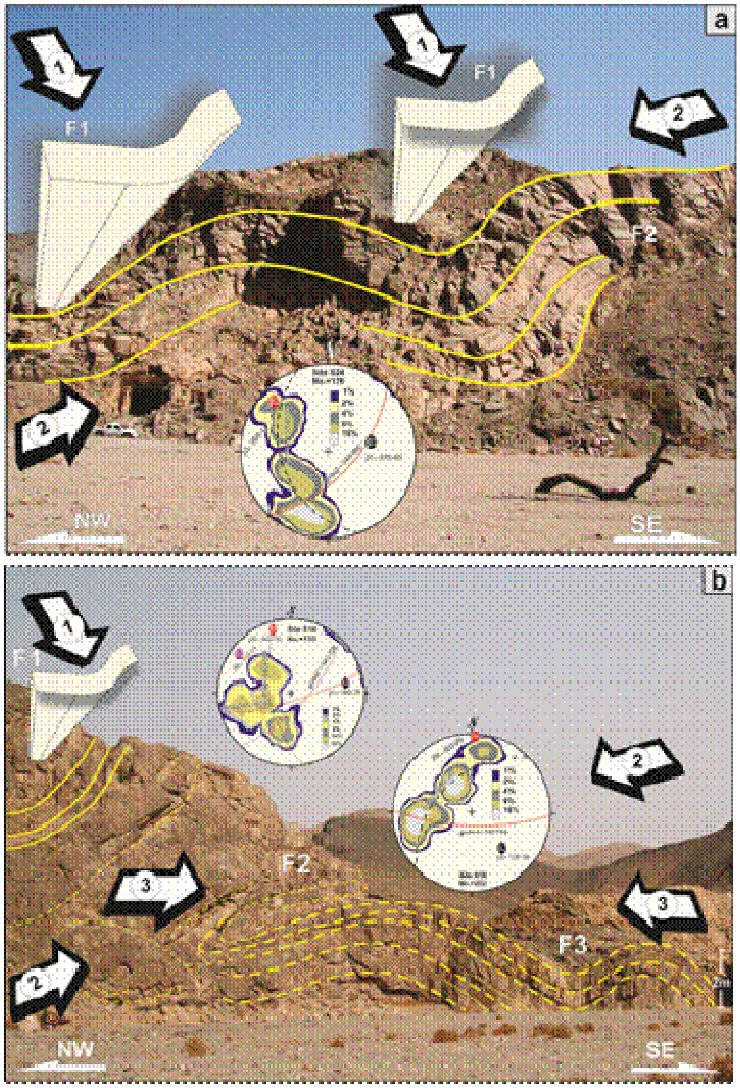


**Figure 6.** Fold interference pattern showing the impact of NW-SE folding; (a), E-W then NW-SE folding. (b), NW-SE thrusts and/or strike-slip faults on the E-W and NW-SE sets of folds. Remark the impact of these sequences of folds shown on the density-contoured lower hemisphere Schmidt net stereograms of structural data, sites; S19 and S24

or the NW-SE sets of folding are earlier to that of the NNW-SSE orientation (Figures 6b and 10a,b), and suggest a third phase of folding (Df3) defined by NNW-SSE oriented fold axes.

### d) Folding around N-S

Folds of fold axes oriented around N-S direction are rarely recorded in the study area. This set has been recorded with almost horizontal axes (Figure 11) especially near granite contacts with mélange. The shape of the folded rock types and their internal structure suggest a fourth phase of folding (Df4) defined by horizontal fold axes oriented around the N-S direction that could be due to the response, accommodation and reorientation of the preexisting structural fabrics to the stresses created during the emplacement of the granitic intrusion.

## Brittle deformation analyses

In the present study, two quantitative approaches were followed. The first depends on field characterization of the conjugate fault system; neoformed or inherited, as well as recording of the relative chronology and their associated features (intra-formational breccias, slumps,

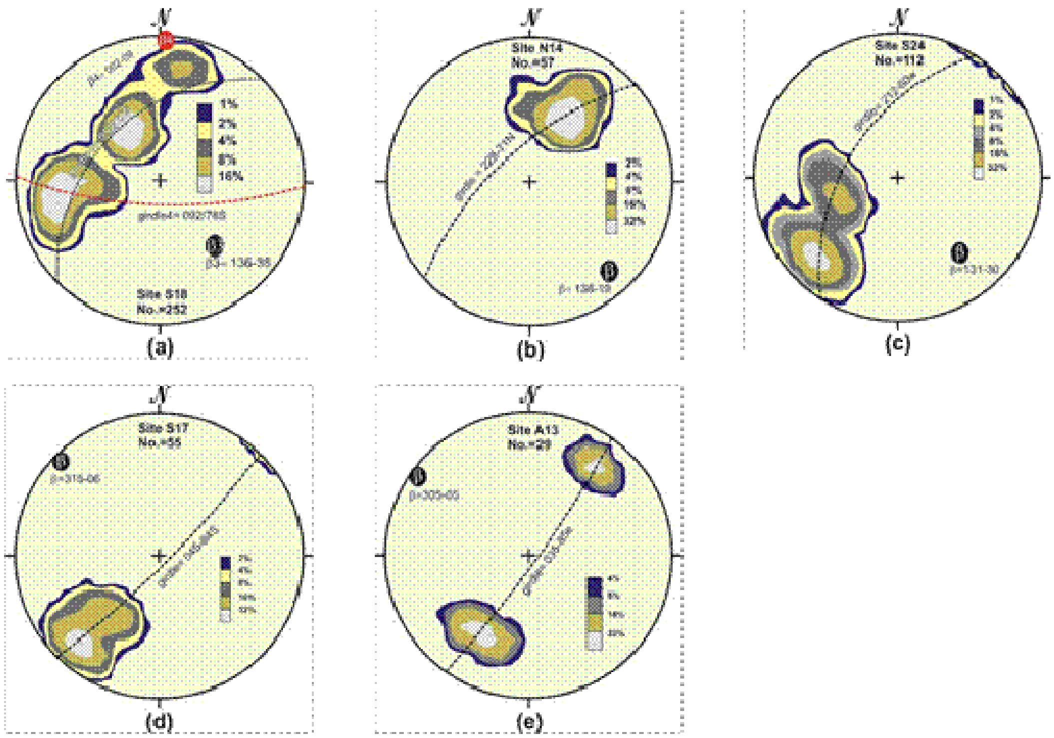


**Figure 7.**Density-contoured lower hemisphere Schmidt net stereograms of structural data from the NSB. Shading for all stereograms are from lowest to highestconcentrations representing poles to foliation measurements reflecting the NW-SE folding; sites A13, N14, S17,S18 and S24. Remark the impact of N-Sfolding (F4), (a) on NW-SE ones

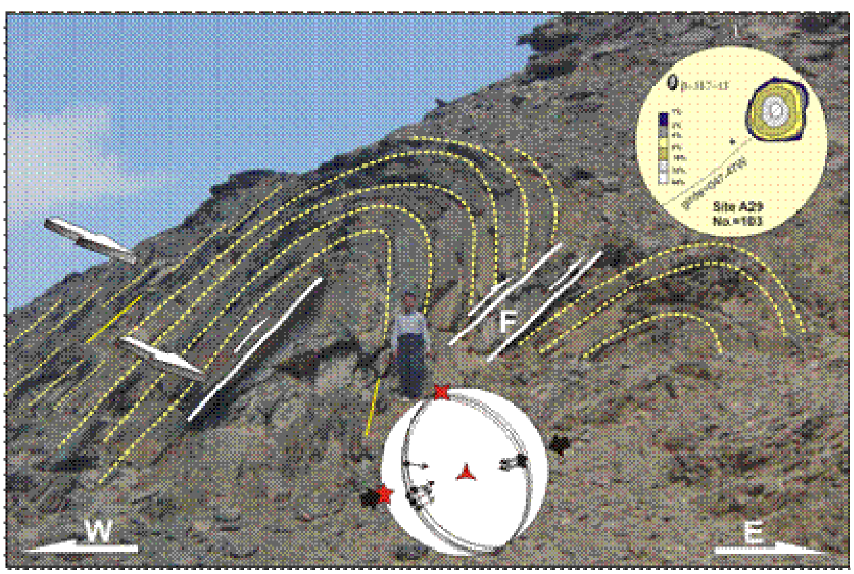


**Figure 8.**Example illustrating the contemporaneous relation between the NW-SE trending axes set of folds and the NW-SE thrust fault system recorded at Abu Rushied area. Remark the parallelism of the fold axis and the bearing of the NW-SE thrust fault system, where the fold axes could be plotted within the NW-SE thrust fault plane, in the same time, the fold axes delineates clearly the plane of the NW-SE thrust fault system

ect.) that give a very good and direct indication about the tectonic regime from the chronological point of view. The second approach is based on the quantitative numerical analysis and treatment of the fault-slip data using the

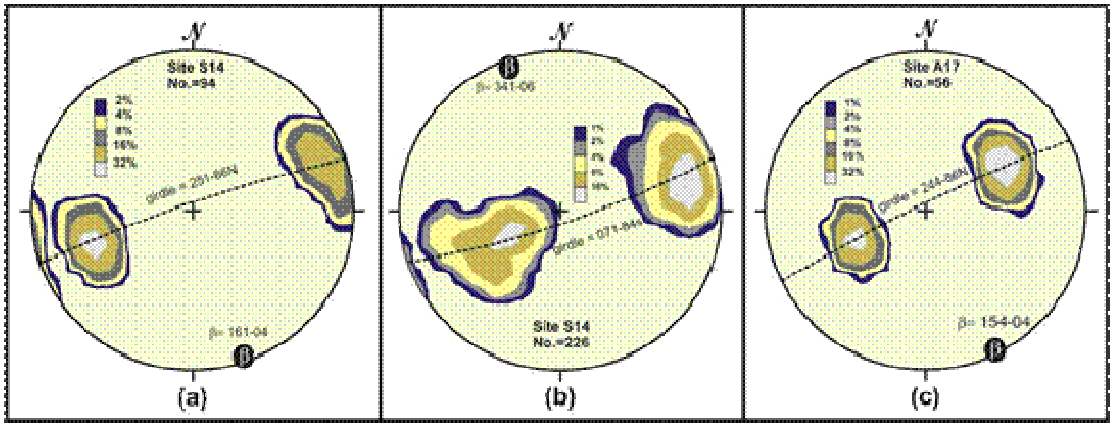


**Figure 9.**Density-contoured lower hemisphere Schmidt net stereograms of structural data from the NSA. Shading for all stereograms are from lowest to highest concentration representing poles to foliation measurements (a, b and c) for the NNW-SSE folding; sites A17 and S14

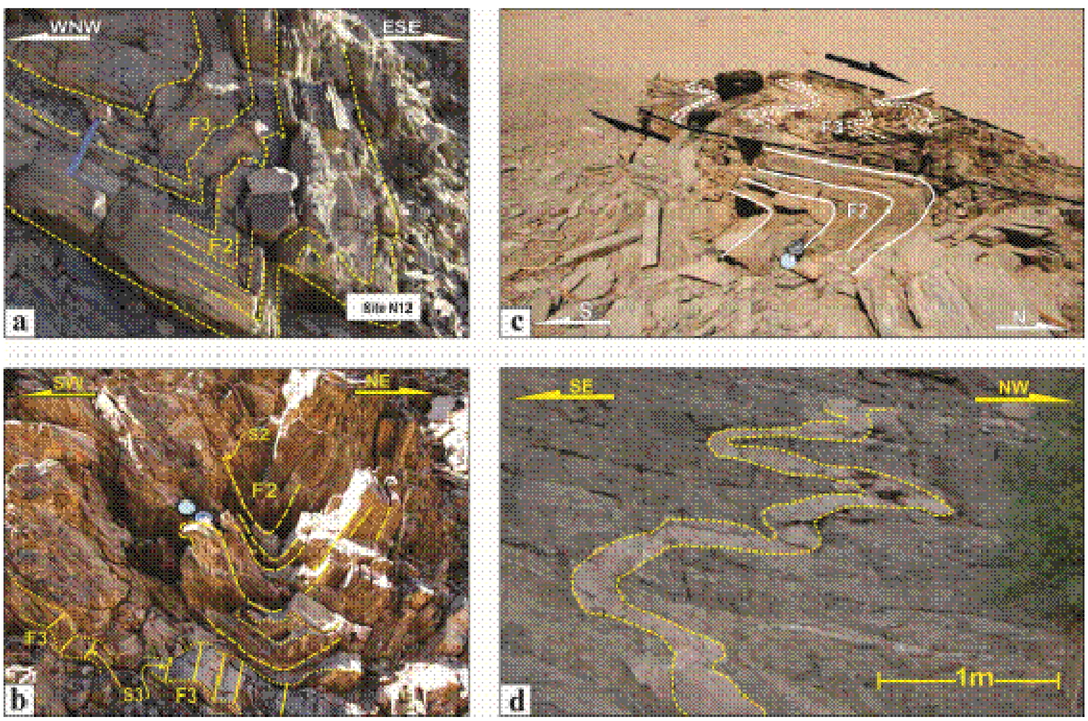


**Figure 10.**Fold interference pattern showing the impact of NNW-SSE folding (F3), (a, b, and c). Remark the zonal kinking (a) as well as, intrafolial NNW-SSE oriented folds axes, folded vein in foliated meta-gabbro with axial planes parallel to the foliation (d)

inversion method, of fault slip data, to compute the paleostress tensor Angelier (1989, 1990 and 1994).

More than 109 sites have been studied in detailed (Figure 2). These sites are distributed almost in all the rock types cropping out in the area so that, 24 sites in metagabbro, 39 sites in mélange, 11 sites in cataclastics, 27sites in monzogranite, 7 sites in muscovite granite and 7sites in alkali feldspar granite. Each site contains several tens of tectonic features measured in small area. It is defined by the coherence and the abundance of fault populations and by the quality of the outcrop.

The quantitative analyses of 8,927 fault slip data sets revealed that more than 539 paleostress tensors (Figures 12-15) such , 51 paleostress tensors are characterizing pure compressional regime, 305strike-slip regime and 183forextensional regime. The calculated tensors characterize, according to their nature, the paleostress regimes and the orientation of the mean stress axes, i.e.

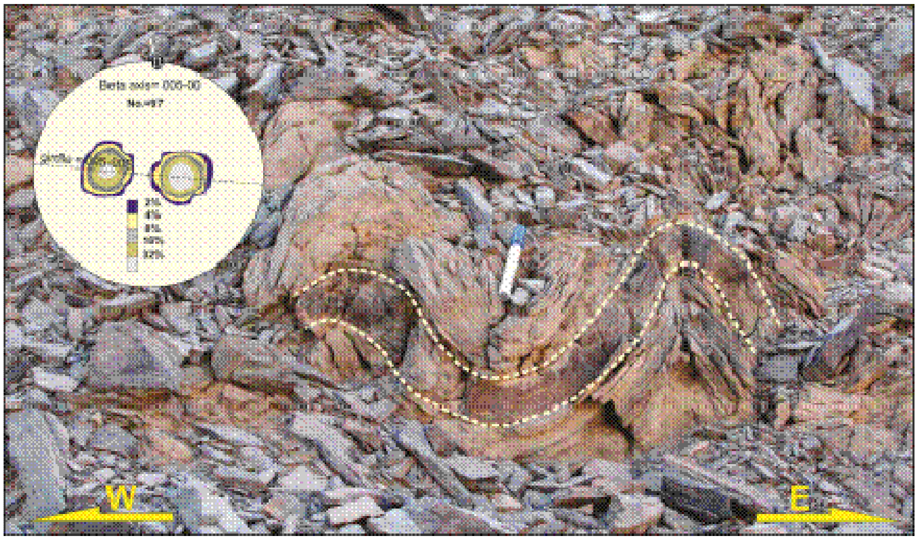


**Figure 11.**Example of the recorded folds with almost horizontal fold axes oriented around the N-S direction, NSB

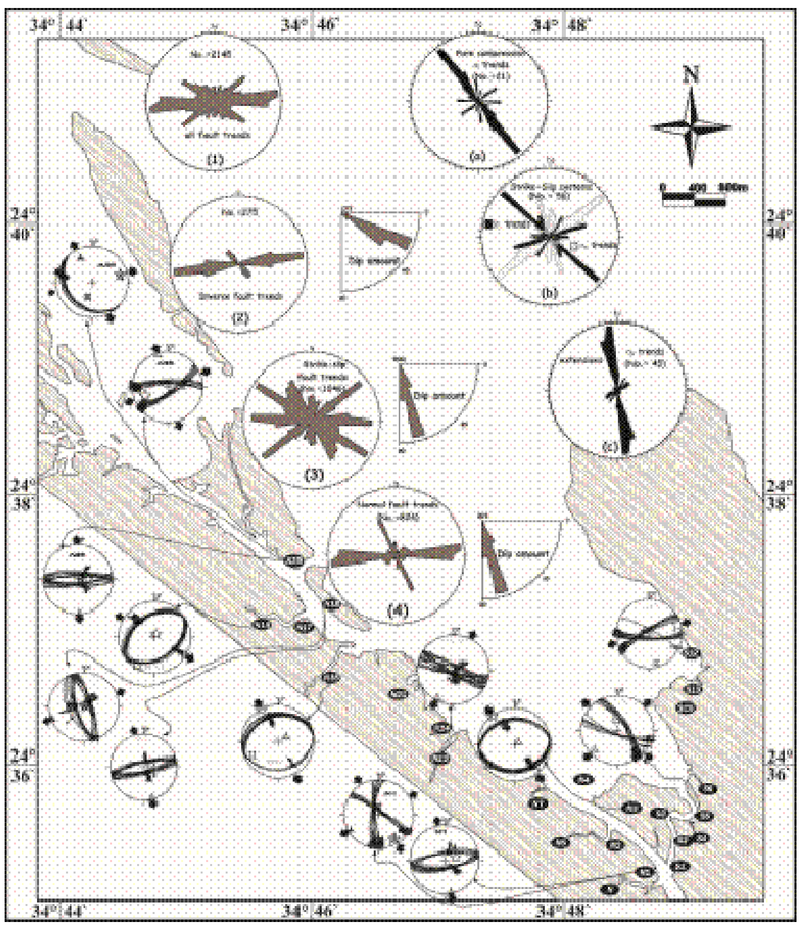


**Figure 12.**Distribution of measurement sites in metagabbro, where the geometrical distribution (in roses) for fault strikes and paleostress tensors measured in metagabbro rock unit. (1)= all fault trends rose, (2) = inverse (thrust) fault analyses, (3) =strike-slip fault analyses and (4) = normal fault analyses. (a)=compression ($\sigma_1$) trends, (b) =strike slip system ($\sigma_1$ and $\sigma_3$) and (c) =extension ($\sigma_3$) as well as examples of the calculated paleostress tensors for some key sites (A35, N1, N2, N3, N16, N18, S5 and S12)

the directions of extension ($\sigma_3$) and/or that of compression ($\sigma_1$). The quantitative analyses of brittle deformations enable us to reconstruct the paleostress field evolution that reflects the regional deformation mechanisms. The calculated paleostress tensors presented in terms of rock types.

**a. Metagabbro paleostress systems**

The analysis of approximately 2,145 fault slip data (275inverse (thrust), 1,046 strike-slip and824 normal) measured in 24 sites throughout the metagabbro revealed 122 paleostress tensors, so that 21 of them correspond to thrust or inverse fault systems, 56 paleostress tensors correspond to strike-slip fault systems and 45 paleostress tensors correspond to normal fault systems (Figure. 12).

The pure compression of thrust fault systems are mainly oriented due to NW-SE and ENE-WSW to E-W (Figure 12, a) whereas, the extensional paleostress tensors are oriented around N-S direction with ENE-WSW to E-W minor trends (Figure 12, c), and the strike-slip fault systems revealed multi-trend pattern (Figure 12, b).

The NW-SE fault systems were recorded at the contacts between the metagabbros and the down thrusted mélange, meta-sediment and cataclastics where the metagabbro is thrusted over them. The field chronological criteria defined later reactivation of the NW-SE trending thrust fault as strike-slip dominated by ENE-WSW trending $\sigma_1$and N-S trending $\sigma_3$(site A35)(Figure 12).

**b. Mélange-meta-sediment paleostress systems**

The analysis of approximately 2,735 fault slip data (280 thrust, 1,529 strike-slips and 926 normal) measured in 38 sites throughout the mélange-metasediment rocks enable the calculation of 178 paleostress tensors, so that 24 of them correspond to thrust fault systems, 96paleostress tensors correspond to strike-slip fault systems and 58 paleostress tensors correspond to normal fault systems (Figure 13).

The pure compression are mainly oriented due to NNW-SSE, NW-SE and ENE-WSW to E-W (Figure13, a) whereas, the extensional paleostress tensors are oriented around N-S direction with NE-SW and ENE-WSW minor trends (Figure 13, c). The strike-slip tensors show multidirectional trends for both ($\sigma_1$) and($\sigma_3$) that could be related to cycles of strike-slip regimes during which almost all the preexisting fault systems have been reactivated as strike-slip ones(Figure 13, b). The geometrical analyses of the thrust fault systems show that the E-W (sites N15 and S17, Figure.13). Moreover, the NW-SE thrust fault systems have been reactivated as strike-slip dominated by NW-SE oriented ($\sigma_1$) and NE-SW oriented ($\sigma_3$). In addition to that, these NW-SE thrust faults show the trace of recent reactivation as oblique slip normal faults (site S11, Figure 13) during an extensional phase of deformation dominated by N-S oriented ($\sigma_3$).

**c. Cataclastic paleostress systems**

The cataclastic exposures enable recording approximately 848 fault-slip data (55 thrust, 407strike-slipsand386 normal) measured in 11 sites. About 55 paleostress tensors have been calculated, so that 6 correspond to thrust faults, 27 correspond to strike-slip faults and 22 correspond to normal faults (Figure 14).

The main compression($\sigma_1$) oriented due to NE-SW to ENE-WSW (Figure 14, a), whereas the strike-slip tensors define WNW-ESE and NW-SE directed ($\sigma_1$) associated with orientations around N-S and NE-SW for ($\sigma_3$)(Figure14, b).The extensional paleostress tensors($\sigma_3$) show permutation around NNW-SSE and ENE-WSW directions with minor NE-SW (Figure 14, c).

The strike-slip system of both ($\sigma_1$ –NW) and ($\sigma_3$ –NE) commonly observed as transpressional sinistral shearing, including top-to-NW oblique-slip shearing with NNE-SSW dextral strike-slip shearing which led to development of the Nugrus-Sikait ductile shear zones. The geometrical analyses of NW-SE to NNW-SSE thrust fault systems reflect a later reactivation in strike-slip regime dominated by NW-SE oriented ($\sigma_1$) and NE-SW oriented ($\sigma_3$)(sites A21, Figure14). In addition to that, the N-Sand E-W normal fault systems (sites A21and A22, Figure14) are lithologically sealed and show tilted geometry restricted only to metasediment-cataclastic reflecting an earlier extensional event dated to the meta-sediment-cataclastic and prior to folding.

**d. Paleostress systems in granitic rocks**

According to detailed field observations, strike-slip and normal faults are the commonly observed fault patterns in the three types of granitic rocks, outcropping at NSB. The approximately 3199 fault slip data (2266 strike-slip and 933 normal) measured in 41 sites throughout the granitic rocks were analyzed (Figure 15).

The biotite monzogranite measurement sites (27) provide 2,114 (446 strike-slip and 175 normal) enable the calculation of 121 paleostress tensors, such89 tensors correspond to strike-slip fault systems and 32 tensors correspond to normal fault systems (Figure 15).

The strike-slip tensors are dominated by NE-SW, E-W and NW-SE oriented ($\sigma_1$) respectively associated with NW-SE, NNE-SSW and NE-SW oriented ($\sigma_3$), while the extensional tensors define N-S and NNE-SSW to NE-SW oriented ($\sigma_3$) (Figure15). The geometrical analyses of the E-W and N-S normal faults (sites A34, N13 and S31, Figure15) reflect later reactivation as oblique slip during NE-SW acting extension ($\sigma_3$).

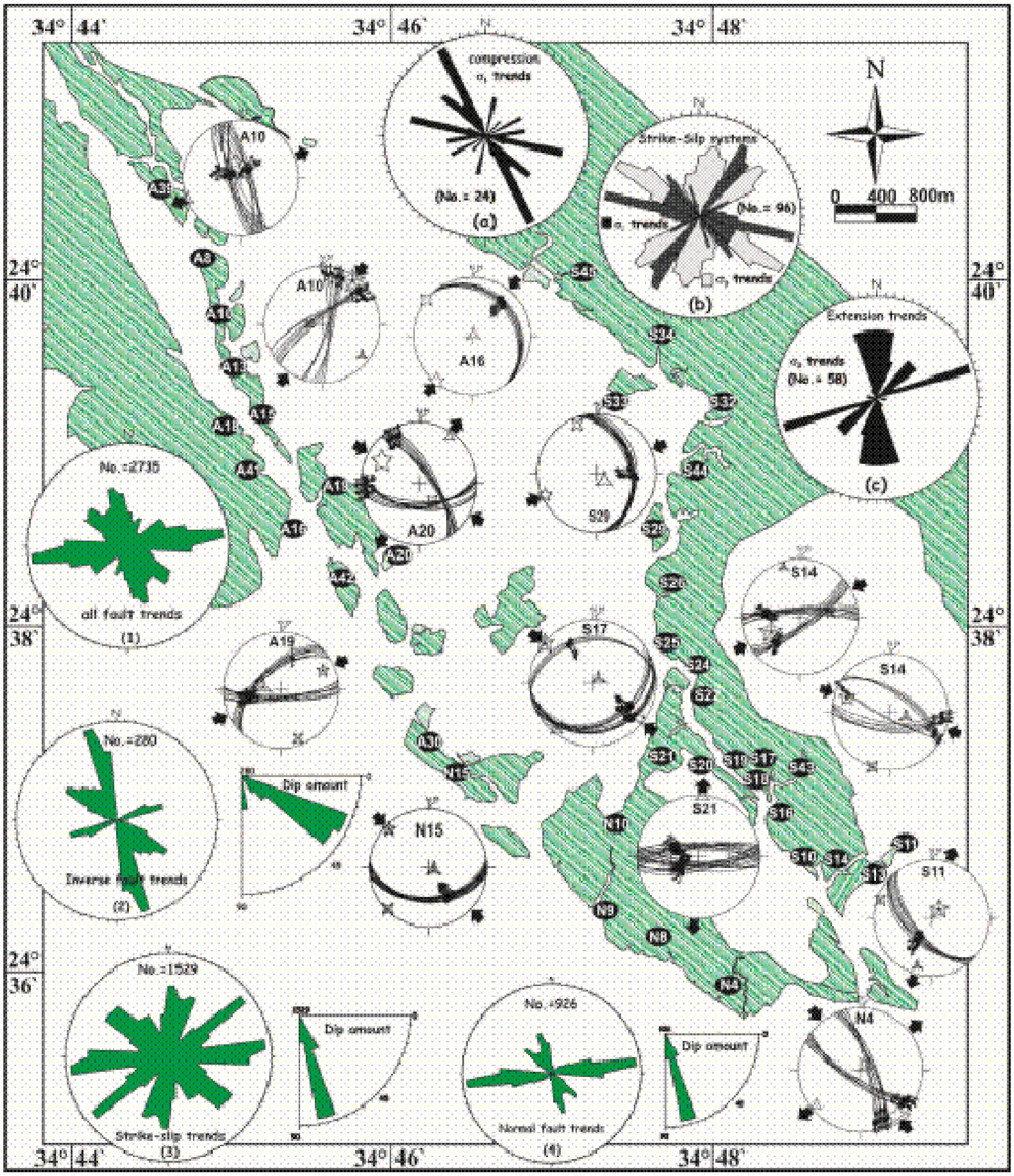

**Figure 13.**Distribution of measurement sites in mélange-metasediments, where the geometrical distribution (in roses) for fault strikes and paleostress tensors. (1)= all fault trends rose, (2) = inverse (thrust) fault analyses, (3) =strike-slip fault analyses and (4) = normal fault analyses. (a)=compression ($\sigma_1$) trends, (b) =strike slip system ($\sigma_1$ and $\sigma_3$) and (c)=extension($\sigma_3$) as well as examples of the calculated paleostress tensors for some key sites(A10, A16, A20, N4, N15, S11, S14, S21 and S29)

The muscovite monzogranite (446 strike-slip and 175 normal faults) as well as the alkali feldspar granite (352 strike-slip and 112 normal faults) fault slip data analysis reveal 37 tensors corresponding to strike-slip faults with almost the same pattern as that obtained from the monzogranite (Figure 15).Moreover, the paleostress tensors corresponding to normal faults (26 tensors) show a clear N-S trending ($\sigma_3$) restricted to the alkali feldspar granite.

## DISCUSSION AND CONCLUSION

Several contributions have been made to the deformation and structural setting of this area,Garson and Krs (1976) considered that Wadi Shait thrust lies within the range of the regional N45º-60ºE block faulting and should be older than the Wadi Nugrus thrust, which lies within the range of deep seated tectonic zones N 30º-35º W. Abdel Khalek and Abdel Wahed (1984) suggest three deformational

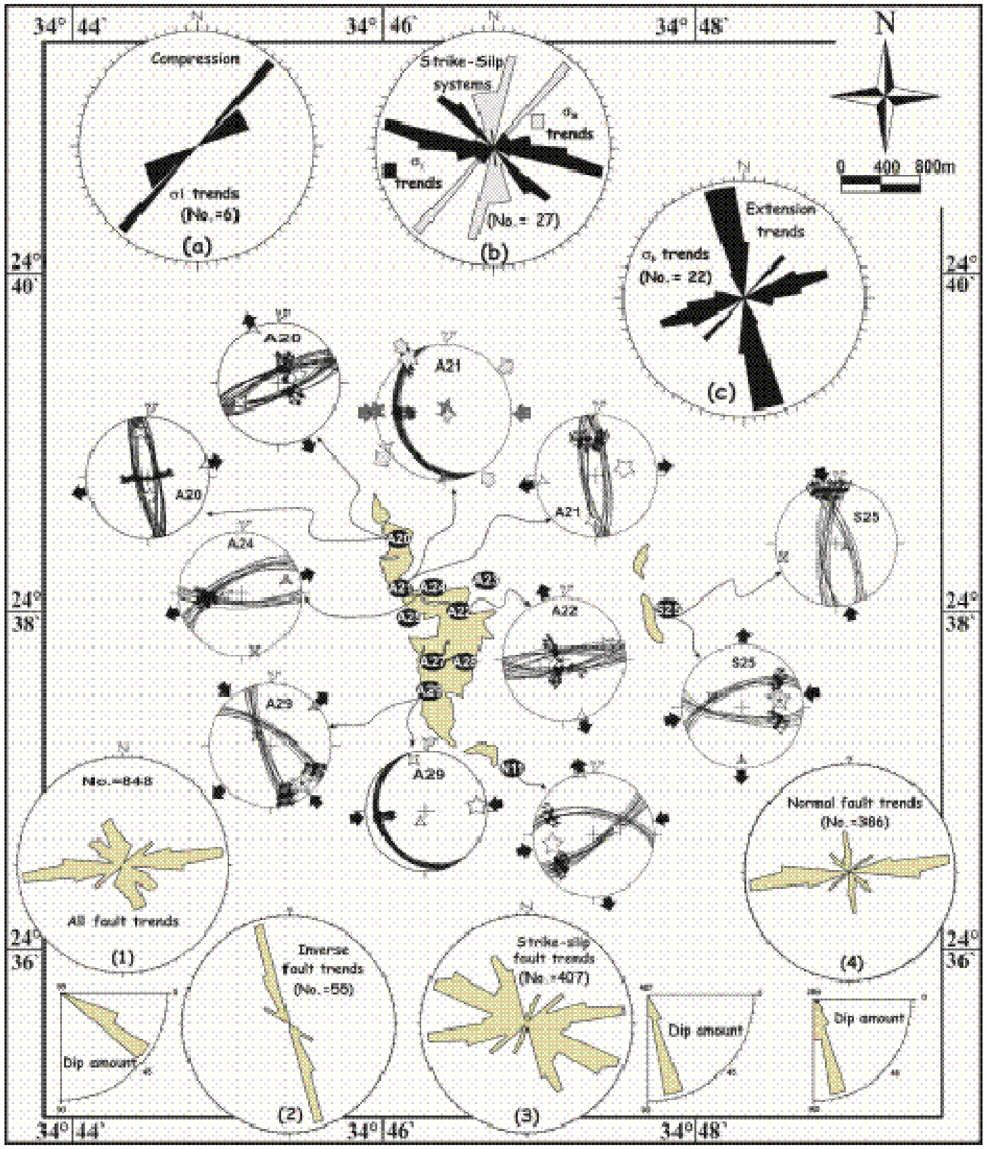


**Figure 14.**Distribution of measurement sites in cataclastics, where the geometrical distribution (in roses) for fault strikes and paleostress tensors. (1)= all fault trends rose, (2) = inverse (thrust) fault analyses, (3) =strike-slip fault analyses and (4) = normal fault analyses. (a)=compression ($\sigma_1$) trends, (b) =strike slip system ($\sigma_1$ and $\sigma_3$) and (c)=extension($\sigma_3$) as well as examples of the calculated paleostress tensors for some key sites(A20, A21, A22,A24, A29, N11 and S25)

phases;d1, d2 and d3. The first deformational phase (d1) is represented by NW-SE axial planes and axes plunging SE and NW respectively. The second (d2) is represented by tight overturned and have SW plunging axes. The third deformational phase (d3) is the weakest in intensity and resulted in open and tight symmetric and asymmetric folds and have NW-SE axial planes. Assaf et al. (2000) stated that the Nugrus –Sikait area involved in superimposed folding events. The F1 folds resulted in isoclined folding and other primary structures around WNW-ESE axes. The F2 folds refolded the F1 folds into upright to overturned and even recumbent folds about NW-SE axes. The F3 folds are of mild intensity compared to the F1 and F2 generations due to NNE-SSW trend.

According to observations in the NSB, the thrust and strike-slip type of faulting that are recorded in metagabbro, ophiolitic mélange and meta-sediments seem to be fold accommodation faults show geometric and kinematics relationship to surrounding folds. In particular, their strikes are generally parallel to the strike of fold axes and they show more or less symmetric arrangement to the axial planes of folds. Moreover, fold structures below and above the thrust plane are almost similar; fold axes can be connected from footwall into the

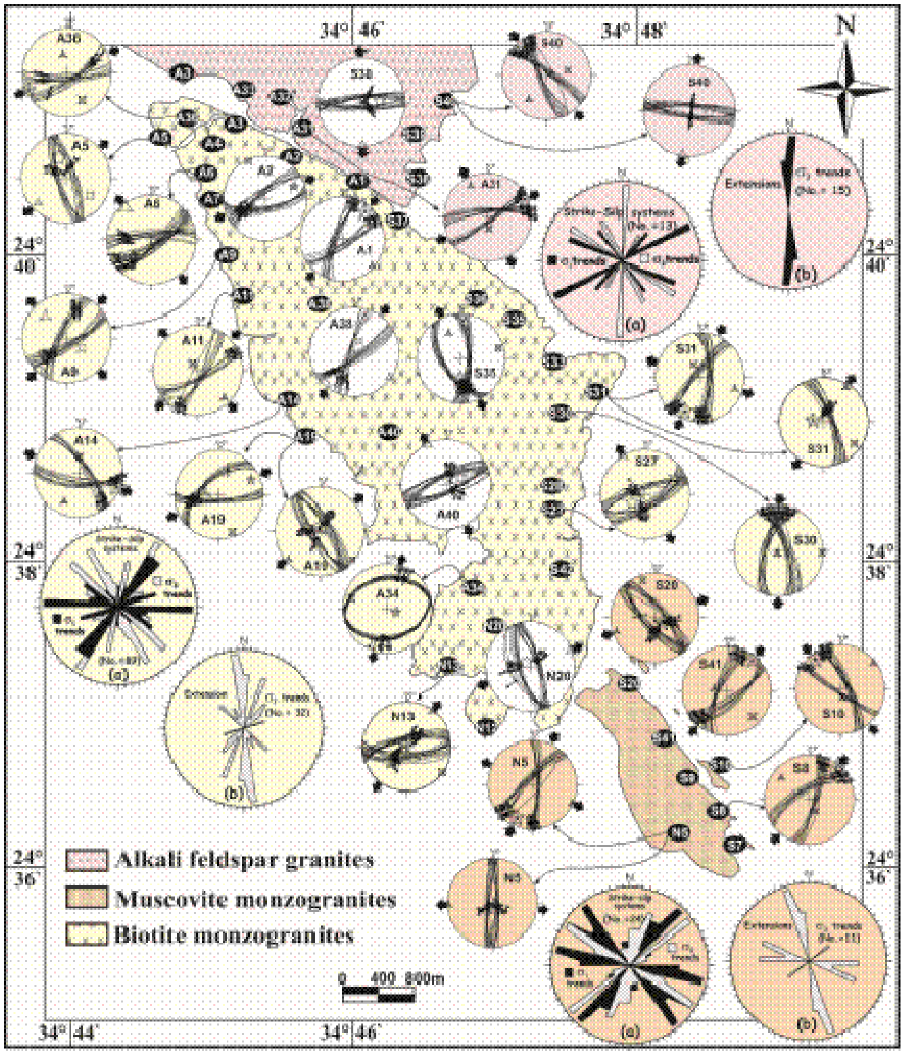


**Figure 15.**Distribution of measurement sites indifferent granitic rocks (biotite monzogranite, muscovite monzogranite and alkali feldspar granite), where the geometrical distribution (in roses) paleostress tensors. (a)=strike slip system ($\sigma_1$ and $\sigma_3$) and (b) =extension ($\sigma_3$) as well as examples of the calculated paleostress tensors for some key sites (A1, A2, A6, A11, A14, A34, N5, N13, N20, S8, S10, S20, S27 and S31

hanging wall block and they may terminate out-of-foliation, i.e. thrust tips form an angle with foliation and do not necessarily run into foliation planes as well as the development of folds with sinistral asymmetry in dextral shear zones.

The fold analyses showed in NSB: an initial planar fabric with E-W trending stretching D1 was folded around older E-W trending Df1 axes then around NW-SE trending Df2 axes followed by regional NE-SW shortening associated with normal upright to overturned folding around NNW-SSE trending Df3 axes. Finally, a fourth phase of folding (Df4) defined by horizontal fold axes oriented around the N-S direction that could be due to the response, accommodation and reorientation of the preexisting structural fabrics to the stresses created during the emplacement of granitic intrusion.

Deformation analysis includes; the paleostress studies (brittle) as well as foliation and fold analyses (ductile) allow proposing a reconstruction of a consistent scheme of tectonic development for the NSB. These analyses indicate that the NSB underwent five distinct episodes of deformation (D1-D5).Summarizing, the major tectonic regimes as follows, from oldest to youngest.

(1)- Pure compression event (D1) with NW-SE to NNW-SSE $\sigma_1$ trend. E-W thrust faulting and forming E-W isoclinal folds (Df1) restricted to meta-gabbros and/or mélange only.

(2)- Pure compression event (D2) with NE-SW to ENE-WSW $\sigma_1$ trend. NW-SE thrust faulting and forming NW-SE folding (Df2) recorded in meta-gabbros, mélange and cataclastics.D1 and D2 are found to be coherent with prograde metamorphism.

.
(3)-Transpressonal sinistral shearing (D3) with NW-SE to NNW-SSE$\sigma_1$ trend including top-to-NW oblique-slip shearing and NNE-SSW dextral strike-slip shearing led to development of the Nugrus-Sikait ductile shear zone and formed NNW-SSE folding (Df3).This event associated with emplacement of granitic intrusions (at leastbiotite and muscovite monzogranite) which cause folding around horizontal N-S direction (Df4).

(4)-Extensional event (D4) with NE-SW to ENE-WSW$\sigma_3$ trend deformation probably related to exhumation of the complex and is characterized by NNW-SSE normal faulting and strike-slip within extensional context.

(5)- Extensional event (D5) with NNW-SSE to N-S $\sigma_3$ trend restricted to the alkali feldspar granite. ENE-WSW to E-W normal faulting, this event associated with emplacement of post granitic dikes and veins.

The tectonic evolution of the NSB can place important insights into a proposed tectonic model suggesting a back-arc basin tectonic environment. The basin was formed as faulted bounded basin controlled mainly by E-W and N-S trending then the western bloc underwent northeastward-directed rollover, thrusting over and shearing with the western margin of the eastern bloc followed by stress release and faulting within extensional context associated with granitic intrusions. Finally, the prevailing of extension tectonics associated with the initial opening of the Red Sea.

## ACKNOWLEDGEMENTS

This study was supported by Egyptian Nuclear Materials Authority (fieldwork), and Japan MEXT program (PhD scholarship to the first author). We are grateful to all members of Abu Rushied project in Nuclear Materials Authority for they assistance in the fieldwork.

### REFERENCES

Abdel Khalek ML, Abdel Wahed M (1984). Structural setting of Hafafit gneisses, Eastern Desert, Egypt, Abstracts of papers presented at the 5th International Conference of Basement Tectonics, Cairo, Egypt, pp. 8

Angelier J (1989). From orientation to magnitudes in paleostress determination using fault slip data. J. Struct. Geol. 11:37– 50

Angelier J (1990). Inversion of field data in fault tectonics to obtain the regional stress: III. A new rapid direct inversion method by analytical means. Geophys. J. Int. 103:363– 376.

Angelier J (1994). Faults slip analysis and palaeostress reconstruction. In: Hancock, P.L. Continental Deformation. Pergamon, Tarrytown, NY, 4:53– 100

Assaf HS, Ibrahim ME, Zalata AA, El- Metwally AA, Saleh GM (2000). Polyphase folding in Nugrus-Sikeit area south Eastern Desert, Egypt. JKAW: Earth Sci., 12:1-16.

Basta EZ, Zaki M (1961). Geology and mineralization of Wadi Sikait area, south Eastrn Desert, J. geol. U. A. R., 5(1):1-38

El Bayoumi RMA (1984). Ophiolites and mélange complex of Wadi Ghadir, Eastern Desert, Egypt. Bull. Fac. Earth Sci., King Abdul Aziz Univ., Jeddah, 6:324-329

El Gaby S (1983). Architecture of the Egyptian basement complex. 5$^{th}$Int.Conf. On Basement tectonics, Egypt

El Gaby S, El-Nady OM, Khudeir AA (1984). Tectonic evolution of the basement complex in the CED of Egypt. Geol., Rundsch 73:1019-1036

El Gaby S, List FK, Tehrani R (1988). Geology, evolution and metallogenesis of the Pan-African belt in Egypt. In: S. El Gaby and R. O. Greiling (eds), The Pan-African Belt of northeast African and adjacent areas, Fried. Vieweg and Shon, Braun Schweig, Wiesbaden, pp. 17-68

El Ramly MF, Akaad MK (1960). The basement complex in the central Eastern Desert of Egypt between latitudes 24° 30 and 25° 4^N Geol. Surv. Egypt, paper 8:35.

El Ramly MF, Greilling RO, Kroner A, Rashwan AA (1984). On the tectonic evolution of the Wadi Hafafit area and environs. EastertDesert of Egypt. Fac. Earth Sci.. king AbdulazizUniv., Jeddah, Saudia Arabia, Bull. 6:113-126.

El Ramly MF, Greilling RO, Kröner A, Rashwan AA, Rasmy H (1993). Explanatory note to accompany the Geological and Structural maps of Wadi Hafafit area. Eastern Desert of Egypt. Geological Survey of Egypt. Paper 68:53.

El Shazly EM, Hassan MA (1972). Geology and radioactive mineralization at Wadi Sikait-Wadi El-Gemal area. South Eastern Desert, Egypt. J. Geol. 16(2):201

El-Filali IA, Hassan MA, Hashad AH (1993). Significance of some mantled gneiss domes in the Arabian- Nubian shield. Ann, Geo. Surv., Egypt. V(XIX):33 – 46.

Fowler A, El Kalioubi B (2002). The Migif-Hafa.t gneissic complex of the EgyptianEasternDesert: fold interference patterns involving multiply deformed sheath folds. Tectonophysics 346:247–275.

Garson MS, Krs M (1976). Geophysical and geological evidence of the relationship of Red Sea traverse tectonic to ancient fractures, Geol. Soc. Am. Bull., 87: 169-181.

Hashad AH, Hassan MA (1959). Report on the prospection work carried out in Wadi El Gemal area, south Eastern Desert, Egypt. Internal Report, AEE, Cairo, UAR.

Hashad AH, Hassan NA (1979). On the validity of an ensimatic island arc cratonization model to the evolution of the Egyptian shield, Ann. Geol. Surv., Egypt, IX : 70 –90.

Hashad AH, Sayyah TA, El-Kholy SB, Youseff A (1972). Rb – Sr isotopic age determination of some basement Egyptian granites, Egypt. J. Geol. V(16):269-281

Hassan MA (1964). Geology and petrographical studies of the radioactive minerals and rocks in Wadi Sikait- Wadi El Gemal area. EasternDesert, U. A. R: M. Sc thesis faculty of science, CairoUniv. Pp. 165

Hassan MA (1973). Geology and geochemistry of radioactive columbite-bearing psammitic gneiss of Wadi Abu Rusheid. South Eastern Desert, Egypt: Annals of Geol. Surv. Egypt. V(III):207-225

Hegazy HM (1984). Geology of Wadi El Gemal area. Eastern Desert, Egypt. Ph. D. Thesis, Assiut Univ., Egypt. Pp. 271

Hilmy ME, El Bayoumi RM, Eid AS (1990). Geology geochemistry, and mineralization of the Psammitic gneiss of Wadi Abu Rushied, Eastern Desert, Egypt. J. Afr. Earth Sci., v (11): 197-205.

Ibrahim ME, Abd El-Wahed AA, Rashed MA, Khaleal FM1, Mansour GM, Watanabe K (2007a). Comparative study between alkaline and calc-alkaline lamprophyres, Abu Rusheid area, south Eastern Desert, Egypt. The 10$^{th}$ Inter. Min., Petrol., and Metall. Eng. Conf., Assuit univ., pp. 99-115

Ibrahim ME, Amer TE, Saleh GM (1999). New occurrence of some nuclear materials and gold mineralization at Wadi Sikait area, south Eastern Desert, Egypt. First seminar on Nuclear Raw Materials and their technology, Cairo, Egypt, pp. 271-284

Ibrahim ME, Assaf HS, Saleh GM (2000). Geochemical alteration and spectrometric analyses in Abu Rusheid altered uraniferous gneissose granites, South Eastern Desert, Egypt Chem. Erde 60:173-188.

Ibrahim ME, Saleh G, Rashed M, Watanabe K, Motomura Y (2006). Epithermal Base metal mineralization in Lamprophyre, south Eastern Desert, Egypt. El Emarat Conf. Geol., Abst., pp. 211.

Ibrahim ME, Saleh GM, Hassan MA, El Tookhi, Rashed MA (2007). Geochemistry of lamprophyres bearing uranium mineralization, Abu Rusheid area, south Eastern Desert, Egypt. The 10$^{th}$ Inter. Min.,

petrol., Metall. Engin, Conf., AssuitUniv.
Ibrahim ME, Saleh GM, Hassan MA, El-Tokhi MM, Rashed MA (2007b). Geochemistry of lamprophyres bearing uranium mineralization, Abu Rusheid area, south Eastern Desert, Egypt. The 10th Inter. Min., Petrol., and Metall. Eng. Conf., Assuit univ., pp. 41-55
Ibrahim ME, Saleh GM, Ibrahim IH, Azab MS, Khamies AA, Oraby F, Abu El-Hassan EA Ragab AA (2004). Geologic and ground spectrometric prospecting of the Abu Rusheid-Sikeit shear zones, South Eastern Desert, Egypt. 7th Arab Conference on the Peaceful Uses of Atomic Energy, Sanaa,Yemen.
Marshak S, Mitra G (1988). Basic methods of structural geology. Prentice Hall Inc., New Jersey, pp. 446
Rashed MA (2005). Geologic studies on a new occurrnce of nuclear materials in Abu Rusheid area, South Eastern Desert, Egypt. Ph. D. Thesis, MansouraUniv. (Demitta), pp. 139
Sabet AH, Tsogoev VB, Bordonosov VP, Shoblovsky RG, Kossa M (1976). On the geologic structures, laws of localization and prospects of Abu Rushied rare metals deposit Annals. Geol. Surv. Egypt. V (VI):181-197
Saleh GM (1997). The potentiality of uranium occurrences in Wadi Nugrus area, south Eastern Desert, Egypt. Ph. D. Thesis Mans. Univ. pp. 171
Stern RJ (1981). Petrogenesis and tectonic setting of late Precambrian ensimatic volcanic rocks, Central Eastern Desert of Egypt. Precambrian Research, 16: 195-230.

How to cite this article: Ibrahim WS, Mostafa MS, Ibrahim ME, Watanabe K and Soliman FA (2014). Deformation history of Nugrus- Sikiat Belt, South Eastern Desert, Egypt; implication for Tectonic Environment. Int. Res. J. Geo. Min. 4(3): 84-100